How are the ready and unready states of nickel–iron hydrogenase activated by H_2? A density functional theory study†

Prabha Jayapal, Mahesh Sundararajan, Ian H. Hillier* and Neil A. Burton

Received 7th June 2006, Accepted 17th July 2006
First published as an Advance Article on the web 27th July 2006
DOI: 10.1039/b608069c

We have explored possible mechanisms for the formation of the catalytically active Ni_a–S state of the enzyme, nickel iron hydrogenase, from the Ni_r^* (ready) or Ni_u^* (unready) state, by reaction with H_2, using density functional theory calculations with the BP86 functional in conjunction with a DZVP basis set. We find that for the reaction of the ready state, which is taken to have an –OH bridge, the rate determining step is the cleavage of H_2 at the Ni^{3+} centre with a barrier of $\sim$15 kcal mol^{-1}. We take the unready state to have a –OOH bridge, and find that reaction with H_2 to form the Ni_r–S state can proceed by two possible routes. One such path has a number of steps involving electron transfer, which is consistent with experiment, as is the calculated barrier of $\sim$19 kcal mol^{-1}. The alternative pathway, with a lower barrier, may not be rate determining. Overall, our predictions give barriers in line with experiment, and allow details of the mechanism to be explored which are inaccessible from experiment.

Introduction

Non-heme iron enzymes are ubiquitous in biology and have important applications in various fields.[1,2] One such group of enzymes are the hydrogenases which are currently of great interest in view of their possible future use as fuel cells.[3–5] Hydrogenases are found both in prokaryotes and eukaryotes where they catalyse the inter-conversion between H_2 and protons.[5]

There are three classes of hydrogenase, [Fe–Fe] hydrogenases[6] (formally called [Fe]- or Fe-only hydrogenases) with two Fe atoms in the active site, [Ni–Fe] hydrogenases which contain a Ni and an Fe atom at the active site,[7] and [Fe]–hydrogenases that have a single Fe atom[8] (formerly called 'metal-free' hydrogenase, whose structure is yet to be characterized crystallographically). Both Fe–Fe and Ni–Fe hydrogenases have at least one carbon monoxide as a ligand bound to Fe, and may also have one or more cyanide ligands similarly bound (Fig. 1). The [Fe–Fe] and [Ni–Fe] hydrogenases also contain Fe–S clusters, which act as an electron source and sink.[9–11]

The first X-ray structure of a [Ni–Fe] hydrogenase was of the oxidized form of *D. gigas*.[9,12] Subsequently, X-ray structures for the oxidized form (*D. fructosovorans*,[13,14] *D. vulgaris* (Miyazaki)[15]) and for the reduced form (*Dm. baculatum*,[16] *D. vulgaris*[17]) have been reported. A surprising feature of the Ni–Fe cluster are the two CN and one CO ligands bound to iron, identified by IR spectroscopy.[12] It has been suggested that *D. vulgaris* involves an alternative sulfoxide (SO) ligand.[17] In the [Ni–Fe] hydrogenases there are four cysteine (Cys_{65}, Cys_{68}, Cys_{530} and Cys_{533}, in *D. gigas*) derived ligands, two being metal bridging (Cys_{68} and Cys_{533}), the remainder being terminal nickel ligands. There has been much speculation as to the reaction pathway for hydrogen reduction within the dimetallic cluster, and the role of residues such as the conserved glutamic acid (Glu_{18}) whose essential role has been identified by mutagenesis studies.[18]

The [Ni–Fe] hydrogenases have been extensively studied by X-ray crystallography, spectroscopy (particularly EPR, ENDOR and IR) and by electrochemical techniques, in order to unravel the quite complex catalytic cycle.[9,12–22] It is generally accepted that there are two catalytically inactive forms, that are EPR active, and are labelled "unready" (Ni_u^* or Ni–A) and "ready" (Ni_r^* or Ni–B), in which the Ni ion is in the oxidized state (Ni^{3+}, Fe^{2+}).[23] Reduction at the nickel centre gives at least three redox states of the Ni–Fe cluster that are believed to be directly involved in catalysis. These have been labelled Ni_a–S (or Ni–SI), Ni_a–C^*, and Ni_a–SR (Ni–R). The relationship between the inactive and active cycle is shown in Scheme 1.

Experimental studies of [Ni–Fe] hydrogenases have shown that the ready state is activated by molecular hydrogen or by low-potential electron donors within a few seconds, whilst the activation of the unready state by H_2 takes several hours.[23,24] Each of these inactive states contains an atom, or small group (X) which bridges the Ni and Fe atoms and prevents catalysis. The identification of the precise nature of X presents experimental problems, and is presently not totally resolved, but small oxygen-containing species are generally favoured, in line with the loss of catalytic activity of the active states upon the addition of O_2.[25] An exception to this is the enzyme from *D. vulgaris* (Miyazaki) for which an exogenous sulfur-containing ligand, released as H_2S upon activation, has been proposed.[15] However, it has been suggested that even this enzyme

School of Chemistry, University of Manchester, Manchester, UK M13 9PL. E-mail: ian.hillier@manchester.ac.uk; Fax: +44 (0) 161 275 4734; Tel: +44 (0) 161 275 4686

† Electronic supplementary information (ESI) available: Optimized Cartesian coordinates (Å) and zero point corrected energies (Hartrees) of the molecules studied in this paper. Imaginary frequencies (cm^{-1}) for the transition states are given in parentheses. See DOI: 10.1039/b608069c

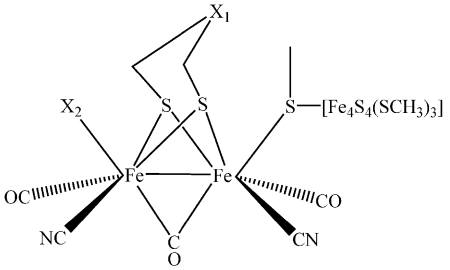

(i) Fe–Fe hydrogenase, where X_1 can be N, O or C and X_2 is CO, H_2 or vacant

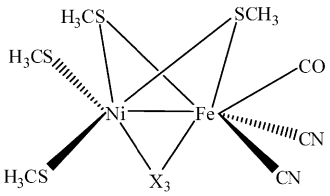

(ii) Ni–Fe hydrogenase, where X_3 can be –OH, –OOH, H_2O, $–H^-$ or CO

Fig. 1 Active site structures of (i) Fe–Fe and (ii) Ni–Fe hydrogenase.

may contain an oxygenic species,[21] George *et al*. proposing a bridging OH group in the ready state and a partially reduced O_2 in the unready state.[26] Recently, Volbeda *et al*.[10] and Ogata *et al*.[27] have reported a crystal structure for the unready state and suggest hydroperoxide to be the bridging ligand.

Previous computational studies have focused mainly on the catalytic reaction mechanism itself, and have contributed to an understanding of the structures and actual spin states of the intermediates involved in the reaction cycle, as well as their spectroscopic properties. In particular, Hall and co-workers have shown how the vibrational frequencies of the CO and CN ligands are a good probe of the electronic structure of the di-metal core.[28,29] Siegbahn *et al*. have reviewed a number of possible reaction pathways predicted by density functional theory (DFT), by which di-hydrogen is cleaved at the iron atom in the catalytic cycle.[30] Fan and Hall,[31] and Bruschi *et al*.[32] have investigated the problem of defining the spin state of the nickel atom (Ni^{2+}) in the reduced state. By comparing measured and computed EPR hyperfine tensors, Lubitz and coworkers[21] have concluded that OH^- is the bridging group in Ni_r^* but not in Ni_u^*.

We here suggest a number of possible reaction mechanisms whereby the inactive ready and unready states can be transformed into the catalytically active Ni_a–S state, and investigate their credibility by computation of the associated potential energy surfaces.

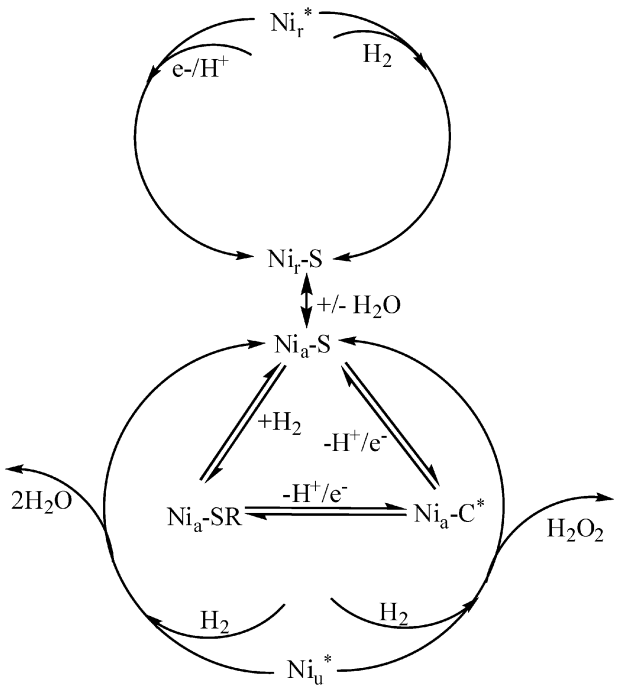

Scheme 1 The relationship between various states of Ni–Fe hydrogenase.

Computational details

In common with most applications of quantum chemical methods to current problems involving transition metal complexes, the size and number of the systems we shall study here precludes the use of *ab initio* methods which explicitly include a high level of electron correlation. We therefore resort to the use of DFT methods and faced with the choice of functional and basis set, have decided to use the BP86 functional[33,34] in conjunction with the DZVP basis.[35] This functional was recently used by Zampella *et al*.[36] to investigate the H_2 activation of synthetic model complexes of Ni–Fe hydrogenase and gave good correlation with structural data. In addition this basis set gives results consistent with the experimental spin densities (derived from EPR) for Ni–Fe hydrogenases.[37]

We have performed geometry optimizations with no constraints using GAUSSIAN 03.[38] All stationary structures have been characterized by calculation of their harmonic frequencies, and it was verified that all transition structures connect the reactants to products by performing an intrinsic reaction coordinate (IRC) analysis.[39,40] A stability check was also carried out on all wavefunctions.[41] Models for the ready and unready states were extracted from the appropriate enzyme structure (PDB code: 2FRV-ready state[12] and 1YQ9-unready state[10]), with the cysteine residue modelled as methyl thiolate ($–SCH_3$). All calculations were performed on the low spin state of Fe and Ni, as previously done by Zampella *et al*. for the synthetic model compounds.[36] All energies have been corrected for zero point effects.

Results and discussion

(a) Activation of the ready state

Both Stein and Lubitz[42] and Kurkin *et al*.[23] have proposed OH^- to be the bridging ligand for the ready state (Ni_r^*) and on the basis of EPR and DFT studies the former proposed that protonation and electron reduction of the Ni_r^* state leads to the Ni_a–S state, and that the bridging H_2O molecule of this state then acts as a base to cleave the di-hydrogen (in the catalytic cycle) forming a hydronium and a hydride ion. Kurkin *et al*.

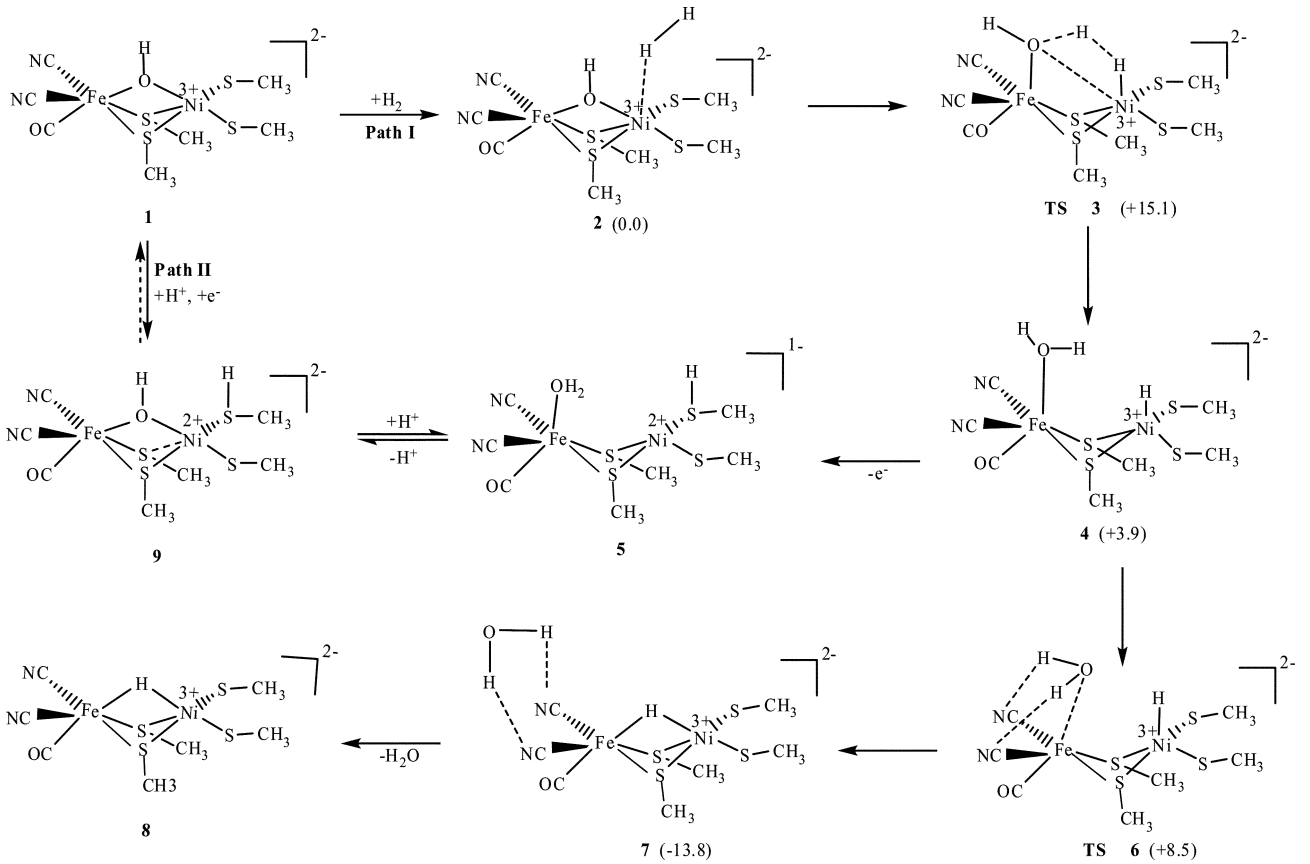

Scheme 2 Proposed reaction mechanisms for the conversion of the Ni_r^* state (**1**) to the Ni_r–S state (**5**). Relative energies (kcal mol^{-1}) of the structures are given in parentheses.

suggest a pathway in which the addition of H_2 to the Ni_r^* state leads to the Ni_r–S state. [23] In this mechanism the bridging –OH group itself cleaves the di-hydrogen to yield H_2O and the hydride ion which leaves as a proton and two electrons, reducing both the Fe–S cluster and the nickel atom (to Ni^{2+}). Based on stopped-flow experiments, they identified that the ready state (Ni_r^*) takes only 6 s to become activated when treated with H_2. With different concentrations of H_2, the development of IR bands at 1950 cm^{-1} and at 1936/1921 cm^{-1} are observed, and are interpreted in terms of the production of both Ni_a–C^* and Ni_r–S states, respectively.[23]

Guided by these previous studies we propose a reaction mechanism for the activation of the ready state shown in Scheme 2, and now describe the results of modelling this process.

In the Ni_r^* state, we have chosen an unprotonated terminal sulfur which is suggested from a comparison of experimental and computed EPR data.[42] This Ni_r^* state (**1**) can be converted into the Ni_r–S state (**5**) *via* two pathways, I and II (Scheme 2), both of which have been suggested on the basis of experimental studies.[23] The first involves the addition of di-hydrogen, and the second involves the protonation of a terminal sulfur and nickel atom reduction.

Our optimized structure of the Ni_r^* state (**1**) is in good agreement with other computational results.[28,42] When compared with experiment[10] (Fig. 2), the Fe–Ni distance is in good agreement, but there are significant differences for the Ni–O and Fe–O values. This could well be due, at least partly, to uncertainties in the experimental values (2.54 Å resolution).

The addition of di-hydrogen to the Ni_r^* state leads to the weakly bound Ni_r^*–H_2 complex (**2**), in which the Fe–Ni distance is essentially unaltered, this species (**2**) being only 0.6 kcal mol^{-1} higher in energy than **1**. The conversion of **2** to the product (Ni_r–S state, **5**) proceeds *via* a transition state (**3**) and an intermediate (**4**). In the transition state, the nickel oxygen bond (of the bridging OH^- group) is broken (3.40 Å), which facilitates the binding of H_2 to nickel. There are two possible transition states for hydrogen molecule cleavage, in which H_2 is bound either side- or end-on to the nickel. The activation energy for the side-on structure is higher than that for the end-on by $\sim$10 kcal mol^{-1}, due to the lack of a second Ni–H bond in the side-on, but not in the end-on structure. In addition, the main geometric change between the side-on and end-on bound transition state is the Ni–Fe distance, which is 3.05 Å in the side-on species, but for the end-on species (**3**) this distance is longer by $\sim$0.3 Å.

The lower energy transition state leads to an intermediate (**4**) with the bound water molecule at the Fe-site and a hydride ion on the Ni-site. Due to the cleavage of the bridgehead in the transition state, the Fe–Ni distance is now increased (3.43 Å). The conversion of this intermediate **4**, which is only

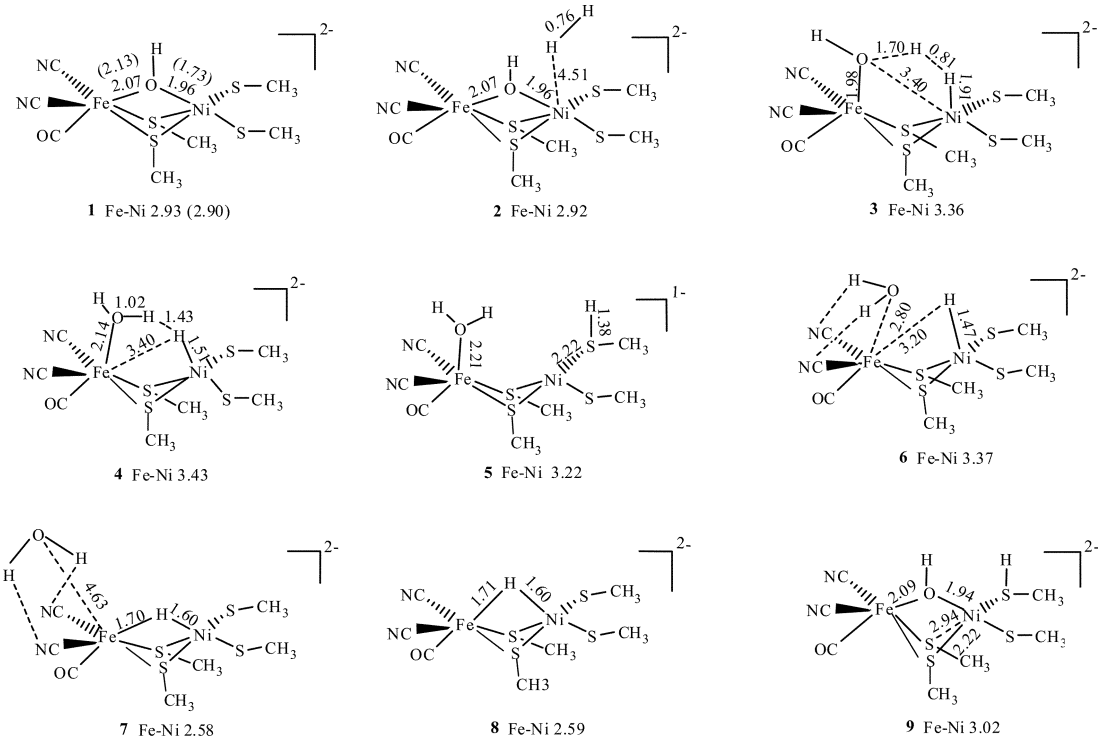

Fig. 2 Bond lengths (Å) for the species involved in the reaction mechanism for the conversion of the Ni_r^* state to the Ni_r–S state. Experimental values are given in parentheses.[12]

3.9 kcal mol^{-1} higher in energy than **2**, to the final Ni_r–S state (**5**) involves the loss of the hydride ion, reduction of the nickel centre, and protonation of the terminal thiolate, with the Fe–S cluster also being reduced. The reduction of the Ni ion and the medial 3Fe–4S cluster has been suggested on the basis of experimental data,[23] and is thus consistent with our proposed pathway. The final Ni_r–S state (**5**) has a bound water molecule which is consistent with experiment.[23] This species will become catalytically active (Ni_a–S) when this water molecule leaves the active site.

Besides the Ni_r–S state (**5**), the intermediate **4** can lead also to a species **7**, which is the precursor to the Ni_a–C^* state (**8**) (Scheme 2) *via* the transition state **6**. Unlike the previous structure (Ni_r–S, **5**), this transition state (**6**), which is 4.6 kcal mol^{-1} higher in energy than **4**, still has a hydride ion bound to Ni but the water molecule is leaving the iron atom, the Fe–O distance being 2.80 Å. This transition structure leads to **7** which has a bridging hydride, as suggested by George *et al.*[26] This species (**7**) is 17.7 kcal mol^{-1} lower in energy than **4**, and has a strong Ni–Fe interaction (2.58 Å), but the water molecule has only a very weak interaction with the Fe centre (4.63 Å). This state (**7**) is finally converted into the Ni_a–C^* state (**8**), when the loosely bound water molecule leaves the pocket.

The second pathway (path II) is the formation of the Ni_r–S state by reduction, *via* the Fe–S cluster, and protonation of the Ni_r^* state (**1**) to give (**9**), where the proton is added to the terminal sulfur of **1**. The main geometric change in this structure is that one of the bridging sulfur to nickel bonds is broken (2.94 Å, Fig. 2) and there is a corresponding lengthening of the Ni–Fe length (3.02 Å). Subsequent protonation of **9** leads to the final product **5**, consistent with the reaction pathways of Stein and Lubitz[42] and Kurkin *et al.*[23]

(b) Activation of the unready state

Stadler *et al.*[43] proposed that both ready and unready states contain a bridging hydroxide, but differ in the way in which the terminal cysteine interacts with the nearby glutamate group. They suggest that the ready, but not the unready, state, has this interaction (H-bond) and also propose that the two states are interconvertible. However, a recent crystallographic study[10] suggests the presence of a –OOH group as the bridging ligand between Ni and Fe in the unready state and this is further supported by Lamle *et al.*[24,44] through electro-kinetic studies. Although these kinetic studies provide mechanistic insights, they cannot provide the corresponding structural information. Our study is the first computational investigation of the conversion of the Ni_u^* state, having a –OOH bridgehead, to the Ni_r–S state.

We start with the model for the Ni_u^* state extracted from the enzyme structure (PDB code: 1YQ9),[10] and propose that it can be converted into the Ni_r–S state *via* two pathways. In path III the bridgehead group finally leaves as hydrogen peroxide (H_2O_2) (Scheme 3a) and path IV involves the cleavage of this group to yield two water molecules as in scheme 3b.

The optimized structure of the Ni_u^* state (**10**) is in good agreement with the X-ray data for the Fe–Ni bond length, but the Ni–O and Fe–O distances are somewhat longer in our

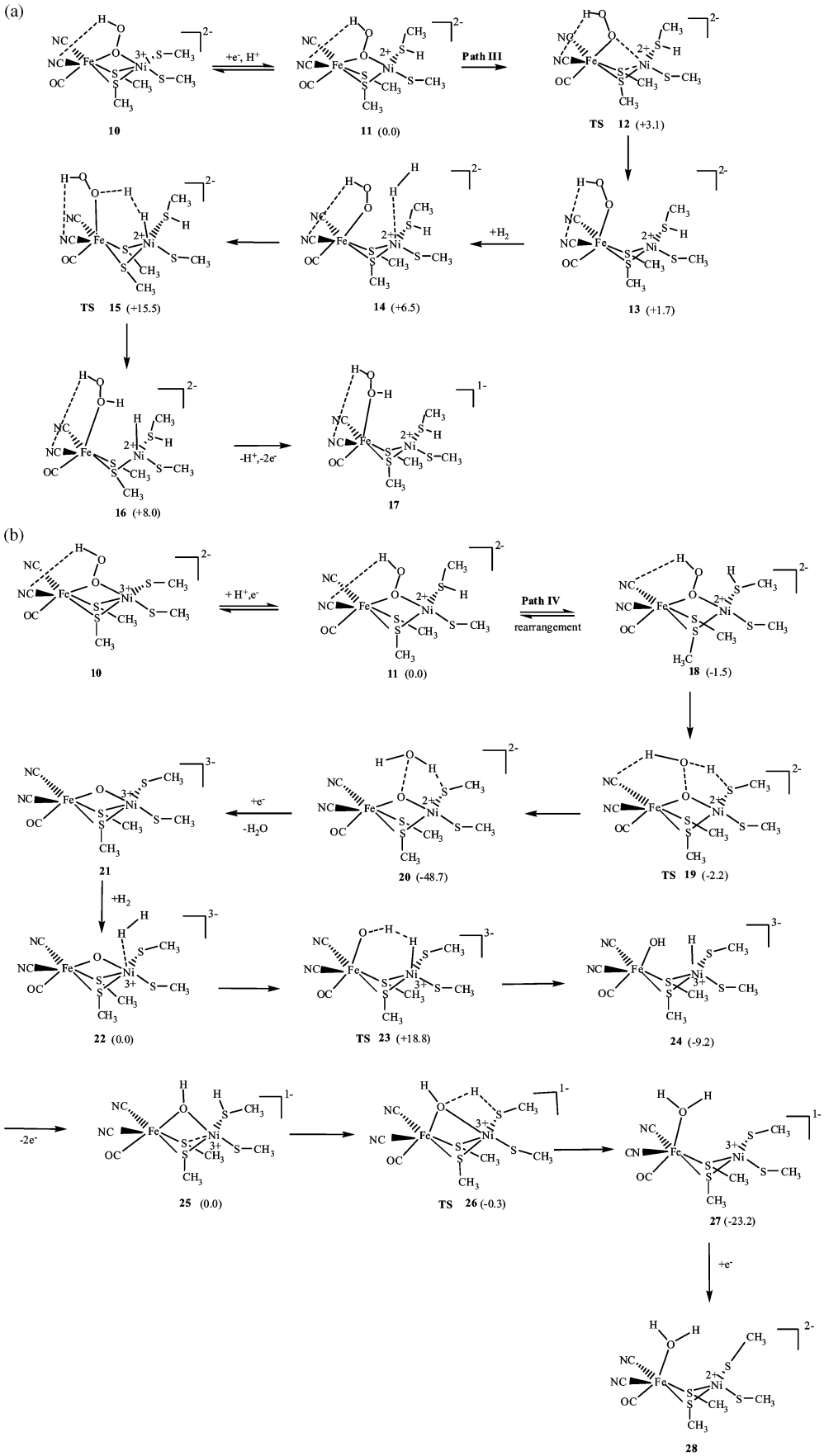

predicted structure (Fig. 3a). This could again be due to the inaccuracy in the low resolution (2.35 Å) crystal structure. The conversion of the Ni_u^* state (**10**) to the Ni_u–S (**11**) state requires one proton and an electron, where the electron reduces the oxidized nickel, and the proton preferentially resides on the terminal sulfur (**11**).[45,46] In the enzyme, Glu_{18} (in *D. gigas*) may donate this proton to the terminal sulfur Cys_{530}, the activity being reduced when Glu is mutated to glutamine (Gln).[18] In this species (**11**) there is a weakened interaction between the Ni and a bridging sulfur atom (3.12 Å). From **11**, there are two possible pathways by which –OOH can be removed either as H_2O_2 (path III in scheme 3a) or cleaved to form two water molecules (path IV in scheme 3b). In pathway III, **11** is converted to **13** *via* the transition state **12** with a barrier of 3.1 kcal mol^{-1} in which the Ni–S (bridging sulfur) bond is formed (2.46 Å) and the Ni–O (of –OOH) bond is broken (2.14 Å, Fig. 3a). This transition state leads to **13** where the Ni–O bond is completely broken (2.70 Å). Addition of di-hydrogen to **13** leads to species **14** in which the di-hydrogen interacts weakly with the nickel atom (3.30 Å). This species is 6.5 kcal mol^{-1} higher in energy than **11** (taking into account the energy of H_2), the bridging Ni–O bond length (of –OOH) being 3.42 Å, (Fig. 3a). Transformation of **14** to **17** proceeds *via* a concerted transition state (**15**) and an intermediate (**16**). In the transition state, the di-hydrogen bond is breaking (1.01 Å) and a new O–H bond (1.26 Å) is being formed. The activation energy for this reaction is 9.0 kcal mol^{-1} which is lower than the experimentally estimated barrier (from electro-kinetics measurements).[24,44] In the transition state, the Fe–Ni bond length is 3.31 Å which is ~0.1 Å shorter than in **14**. The intermediate **16** has an elongated Fe–Ni bond (3.73 Å), a hydrogen peroxide molecule at the iron centre and a hydride ion on the nickel atom. Cleavage of the hydride ion from the intermediate (**16**) as a proton and two electrons (to the Fe–S cluster) leads to the final Ni_r–S state (**17**) which has a Fe–Ni distance (3.25 Å) shorter than that in **16** by ~0.5 Å

In the second pathway (IV), the hydroperoxide ion is cleaved as two water molecules by the consumption of di-hydrogen and a proton from the terminal sulfur (Scheme 3b). Both the cleavage of the peroxide O–O bond and the proton transfer from the terminal sulfur of **11** to form the first water molecule is the first reaction in this pathway (Scheme 3b) and occurs *via* a concerted transition state. In order for the reaction to be facilitated, the –SH should orientate towards the –OOH group as in structure **18**, and this rearranged species is only 1.5 kcal mol^{-1} lower in energy than **11**. In the subsequent transition state (**19**), the Fe–Ni bond length changes only slightly. The water molecule is formed *via* breaking the S–H (1.53 Å) and the O–O (1.65 Å) bonds, and by formation of a new, O–H bond (1.39 Å).

The corresponding activation energy is –0.7 kcal mol^{-1} (without zero point correction this value is 1.2 kcal mol^{-1}) This transition state leads to an intermediate (**20**), where the bridging Ni–S bond is broken (4.00 Å) and the leaving water molecule is hydrogen bonded to the terminal sulfur. The addition of one electron (which could be donated from the Fe–S cluster) and the electron transfer from the nickel to the bridging oxygen leads to the species **21**, where all the bonds are conserved compared to **20** and the Fe–Ni distance is short (~2.88 Å) in agreement with Li and Hall (species 1a in the article).[28] The addition of di-hydrogen to the nickel atom is the next step in the reaction. The di-hydrogen is only weakly interacting with the nickel atom (>4.00 Å) in **22** which is consistent with a previous computational investigation,[42] this structure being slightly lower in energy (0.7 kcal mol^{-1}) than **21**. This oxygen bridged molecule is converted to the hydroxide species *via* a concerted transition state (**23**). In this transition state, the O–H bond is forming (1.53 Å) and some H–H bond elongation occurs (0.84 Å) leaving the hydride ion residing on the nickel atom. The activation energy of this reaction is 18.8 kcal mol^{-1} which is consistent with the experimental barrier of ~21 kcal mol^{-1}.[24,44] The transition state (**23**) leads to another intermediate (**24**) which has a long Fe–Ni distance (3.52 Å) which may be due to the absence of the third bridging ligand. The removal of two electrons (to the Fe–S clusters) from species **24** and a proton shift from the nickel to the terminal sulfur is the next step in the reaction to form **25** (Scheme 3b) which facilitates the bridging of the Fe and Ni atoms by the OH group and leads to a shorter Fe–Ni distance (2.92 Å) the Ni-bridging sulfur bond being partially broken (2.53 Å). The removal of the second water molecule from **25** to yield **27**, occurs *via* the transition state (**26**). In this transition state, the S–H bond is breaking (1.48 Å) and the new O–H bond is forming (1.52 Å), which leads to a weakening of the Fe–O bond (2.11 Å). The newly formed water molecule interacts very weakly with the nickel atom (3.04 Å) in **27** and the addition of an electron to **27** weakens the Fe–O interaction (2.24 Å) further (**28**). This species can abstract a proton from the neighbouring residues to form protonated terminal sulfur as in **5** (Scheme 2, Ni_r–S). Finally, the species **28**, can be activated by the removal of the bound H_2O molecule to form the Ni_a–S state.

Conclusions

We have investigated here how the Ni_r^* (ready) and Ni_u^* (unready) states might be converted into the Ni_r–S state upon H_2 addition, using DFT methods and a cluster model of the enzyme active site. We have estimated the contribution from the rest of the enzyme by using a continuum model (CPCM)[38] with a dielectric of 4.9. We find that the barriers, which are central to our proposed mechanisms, are changed by less than ~3 kcal mol^{-1}, showing that isolated cluster models are appropriate for these systems.

We have explored a series of possible species including a number of transition states on the potential energy surface

Scheme 3 (a) Proposed reaction mechanisms for the conversion of the Ni_u^* state (**10**) to the Ni_r–S state (**17**) *via* removal of H_2O_2. Relative energies (kcal mol^{-1}) of the structure are given in parentheses. (b) Proposed reaction mechanisms for the conversion of the Ni_u^* state (**10**) to the Ni_r–S state (**28**) *via* removal of $2H_2O$. Relative energies (kcal mol^{-1}) of the structures are given in parentheses.

(a)

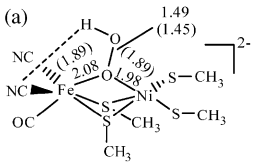

10 Fe-Ni 2.96 (2.91)

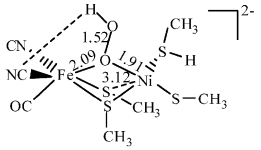

11 Fe-Ni 3.12

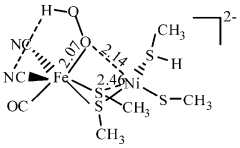

12 Fe-Ni 3.02

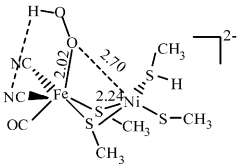

13 Fe-Ni 3.19

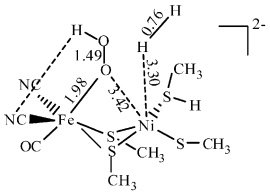

14 Fe-Ni 3.42

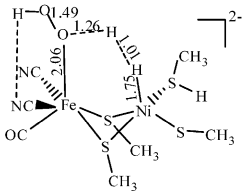

15 Fe-Ni 3.31

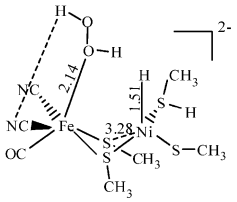

16 Fe-Ni 3.73

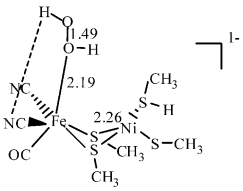

17 Fe-Ni 3.25

(b)

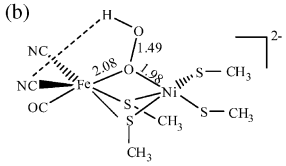

10 Fe-Ni 2.96

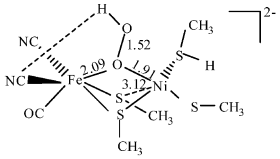

11 Fe-Ni 3.12

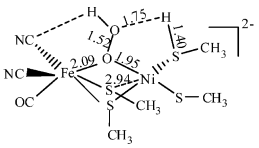

18 Fe-Ni 3.05

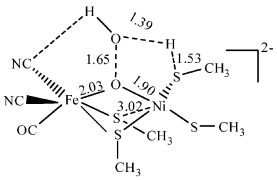

19 Fe-Ni 3.07

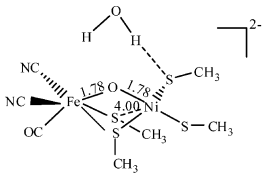

20 Fe-Ni 3.01

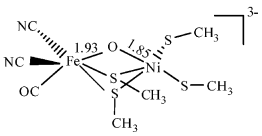

21 Fe-Ni 2.88

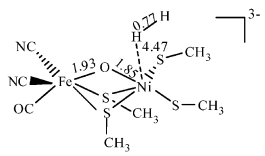

22 Fe-Ni 2.88

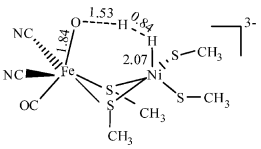

23 Fe-Ni 3.54

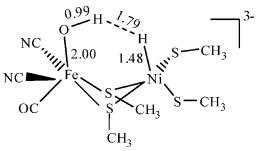

24 Fe-Ni 3.52

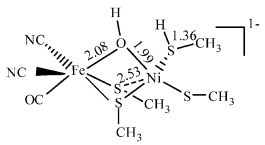

25 Fe-Ni 2.92

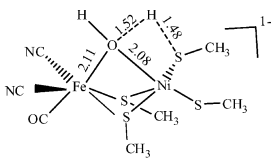

26 Fe-Ni 2.90

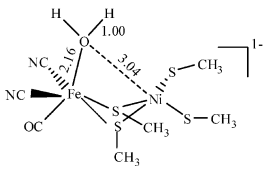

27 Fe-Ni 3.09

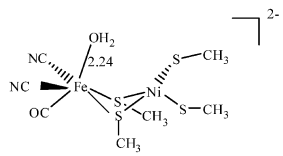

28 Fe-Ni 3.21

involved in these conversions. Our studies of possible pathways is naturally not exhaustive, but our calculations do complement experimental studies and highlight the role of H_2 in these reactions. The major features of our proposed mechanisms are as follows.

(i) The ready state, which is generally agreed to have an –OH bridge, can initially react directly with H_2 followed by a sequence of reactions, to form the Ni_r–S state. The rate determining step, having an activation energy of $\sim$15 kcal mol^{-1}, is the cleavage of H_2 at the Ni^{3+} centre, where reaction with the –OH bridging group leads to the formation of H_2O (Scheme 2, species **3**). Our calculation supports the experimental formation of both the Ni_r–S and Ni_a–C^* state, after the removal of an electron from the intermediate **4**, or formation of the bridging hydride ion to form **8**.

(ii) There is growing evidence that the unready state has a partially reduced dioxygen species as the bridging ligand. We here describe the first computational study of possible mechanisms whereby such a –OOH bridging species can react with H_2 to form the Ni_r–S state. We suggest two pathways for the formation of the Ni_r–S state following reaction with H_2, leading to the formation of either H_2O_2 or two water molecules. These two pathways (path III in Scheme 3a and path IV in Scheme 3b) differ in the actual point in the reaction scheme at which the di-hydrogen reacts, and in the nature of the rate determining step. To form H_2O_2 (path III) H_2 reacts with species **13** formed through the reduction of the Ni_u^* state (**10**) and a transition state (**12**). Here the rate determining step is the cleavage of H_2 at the Ni^{2+} centre and the formation of H_2O_2, this step having a barrier of $\sim$9 kcal mol^{-1}. In the alternative pathway, leading to the reduction of the peroxy species to form two water molecules (path IV), the H_2 molecule reacts with the species **21** having a single bridging oxygen atom. Here the rate determining step again involves H_2 cleavage and O–H bond formation. The corresponding activation energy for this reaction is $\sim$19 kcal mol^{-1} which is very close to an experimental estimate of $\sim$21 kcal mol^{-1}.[24,44] However, path III, which has a considerably lower barrier, may not be the preferred pathway, since here removal of H_2O_2 from the active site may be rate determining.[10] The experimental observation that activation of the unready state by H_2 requires many ($N > 1$) electron transfers is consistent with our path IV scheme which has a number of steps involving electron transfer.[44] Further, both of the two candidates for the Ni_r–S species which arise from path III (**17**), and path IV (**28**), and which differ in the protonation of terminal sulfur, have been suggested to be possibilities for the Ni_a–S state after the removal of H_2O_2 or H_2O molecules.[28,32]

Fig. 3 (a) Bond lengths (Å) for the species involved in the reaction mechanism for the conversion of the Ni_u^* state to the Ni_r–S state *via* removal of H_2O_2. Experimental values are given in parentheses.[10] (b) Bond lengths (Å) for the species involved in the reaction mechanism for the conversion of the Ni_u^* state to the Ni_r–S state *via* removal of $2H_2O$.

References

1 M.-H. Baik, M. Newcomb, R. A. Friesner and S. J. Lippard, *Chem. Rev.*, 2003, **103**, 2385.
2 E. I. Solomon, *Inorg. Chem.*, 2001, **40**, 3656.
3 J. Tye, M. B. Hall and M. Y. Darensbourg, *Proc. Natl. Acad. Sci. U. S. A.*, 2005, **102**, 16911.
4 F. A. Armstrong, *Curr. Opin. Chem. Biol.*, 2004, **8**, 133.
5 R. Cammack, M. Frey and R. Robson, *Hydrogen as a Fuel: Learning from Nature*, Taylor and Francis, London, 2001.
6 C. Tard, X. Liu, S. K. Ibrahim, M. Bruschi, L. De Gioia, S. C. Davies, X. Yang, L.-S. Wang, G. Sawers and C. J. Pickett, *Nature*, 2005, **433**, 610.
7 D. J. Evans and C. J. Pickett, *Chem. Soc. Rev.*, 2003, **32**, 268.
8 E. J. Lyon, S. Shima, G. Buurman, S. Chowdhuri, A. Batschauer, K. Steinbach and R. K. Thauer, *Eur. J. Biochem.*, 2004, **271**, 195.
9 A. Volbeda, M. H. Charon, C. Piras, E. C. Hatchikian, M. Frey and J. C. Fontecilla-Camps, *Nature*, 1995, **373**, 580.
10 A. Volbeda, L. Martin, C. Cavazza, M. Matho, B. W. Faber, W. Roseboom, S. P. J. Albracht, E. Garcin, M. Rousset and J. C. Fontecilla–Camps, *J. Biol. Inorg. Chem.*, 2005, **10**, 239.
11 X. B. Wang, S. Niu, X. Yang, S. K. Ibrahim, C. J. Pickett, T. Ichiye and L.-S. Wang, *J. Am. Chem. Soc.*, 2003, **125**, 14072.
12 A. Volbeda, E. Garcin, C. Piras, A. L. de Lucey, V. M. Fernandez, E. C. Hatchikian, M. Frey and J. C. Fontecilla–Camps, *J. Am. Chem. Soc.*, 1996, **118**, 12989.
13 M. Rousset, Y. Montet, B. Guigliarelli, N. Forget, M. Asso, P. Bertrand and J. C. Fontecilla–Camps, *Proc. Natl. Acad. Sci. U. S. A.*, 1998, **95**, 11625.
14 A. Volbeda, Y. Montet, X. Vernede, E. C. Hatchikian and J. C. Fontecilla–Camps, *Int. J. Hydrogen Energy*, 2002, **27**, 1449.
15 Y. Higuchi, T. Yagi and N. Yasuoka, *Structure*, 1997, **5**, 1671.
16 E. Garcin, X. Vernede, E. C. Hatchikian, A. Volbeda, M. Frey and J. C. Fontecilla–Camps, *Struct. Fold. Des.*, 1999, **5**, 557.
17 Y. Higuchi, H. Ogata, K. Miki, N. Yasuoka and T. Yagi, *Structure*, 1999, **7**, 549.
18 S. Dementin, B. Burlat, A. L. de Lacey, A. Pardo, G. Adryanczyk-Perrier, B. Guigliarelli, V. M. Fernandez and M. Rousset, *J. Biol. Chem.*, 2004, **279**, 10508.
19 F. A. Armstrong and S. P. J. Albracht, *Philos. Trans. R. Soc. London, Ser. A*, 2005, **363**, 937.
20 M. van Gastel, C. Fichtner, F. Neese and W. Lubitz, *Biochem. Soc. Trans.*, 2005, **33**, 7.
21 M. van Gastel, M. Stein, M. Brecht, O. Schroder, F. Lendzian, R. Bittl, H. Ogata, Y. Higuchi and W. Lubitz, *J. Biol. Inorg. Chem.*, 2006, **11**, 41.
22 Q. Wang, J. E. Barclay, A. J. Blake, E. S. Davies, D. J. Evans, A. C. Marr, E. J. L. McInnes, J. McMaster, C. Wilson and M. Schroder, *Chem.–Eur. J.*, 2004, **10**, 3384.
23 S. Kurkin, S. J. George, R. N. F. Thorneley and S. P. J. Albracht, *Biochemistry*, 2004, **43**, 6820.
24 S. E. Lamle, S. P. J. Albracht and F. A. Armstrong, *J. Am. Chem. Soc.*, 2004, **126**, 14899.
25 M. Carepo, D. L. Tierney, C. D. Brondino, T. C. Yang, A. Pamplona, J. Telser, I. Moura, J. J. G. Moura and B. M. Hoffman, *J. Am. Chem. Soc.*, 2002, **124**, 281.
26 S. J. George, S. Kurkin, R. N. F. Thorneley and S. P. J. Albracht, *Biochemistry*, 2004, **43**, 6808.
27 H. Ogata, S. Hirota, A. Nakahara, H. Komori, N. Shibata, T. Kato, K. Kano and Y. Higuchi, *Structure*, 2005, **13**, 1635.
28 S. Li and M. B. Hall, *Inorg. Chem.*, 2001, **40**, 18.
29 S. Niu, L. M. Thomson and M. B. Hall, *J. Am. Chem. Soc.*, 1999, **121**, 4000.
30 P. E. M. Siegbahn, M. R. A. Blomberg, M. Pavlov and R. H. Crabtree, *J. Biol. Inorg. Chem.*, 2001, **6**, 460.
31 H. J. Fan and M. B. Hall, *J. Am. Chem. Soc.*, 2002, **124**, 394.
32 M. Bruschi, L. De Gioia, G. Zampella, M. Reiher, P. Fantucci and M. Stein, *J. Biol. Inorg. Chem.*, 2004, **9**, 873.
33 A. D. Becke, *Phys. Rev. A*, 1988, **38**, 3098.
34 J. P. Perdew, *Phys. Rev. B*, 1986, **33**, 8822.
35 N. Godbout, D. R. Salahub, J. Andzelm and E. Wimmer, *Can. J. Chem.*, 1992, **70**, 560.
36 G. Zampella, M. Bruschi, P. Fantucci and L. De Gioia, *J. Am. Chem. Soc.*, 2005, **127**, 13180.
37 M. Stein and W. Lubitz, *Phys. Chem. Chem. Phys.*, 2001, **3**, 2668.

38 M. J. Frisch, G. W. Trucks, H. B. Schlegel, G. E. Scuseria, M. A. Robb, J. R. Cheeseman, J. A. Montgomery Jr, T. Vreven, K. N. Kudin, J. C. Burant, J. M. Millam, S. S. Iyengar, J. Tomasi, V. Barone, B. Mennucci, M. Cossi, G. Scalmani, N. Rega, G. A. Petersson, H. Nakatsuji, M. Hada, M. Ehara, K. Toyota, R. Fukuda, J. Hasegawa, M. Ishida, T. Nakajima, Y. Honda, O. Kitao, H. Nakai, M. Klene, X. Li, J. E. Knox, H. P. Hratchian, J. B. Cross, V. Bakken, C. Adamo, J. Jaramillo, R. Gomperts, R. E. Stratmann, O. Yazyev, A. J. Austin, R. Cammi, C. Pomelli, J. W. Ochterski, P. Y. Ayala, K. Morokuma, G. A. Voth, P. Salvador, J. J. Dannenberg, V. G. Zakrzewski, S. Dapprich, A. D. Daniels, M. C. Strain, O. Farkas, D. K. Malick, A. D. Rabuck, K. Raghavachari, J. B. Foresman, J. V. Ortiz, Q. Cui, A. G. Baboul, S. Clifford, J. Cioslowski, B. B. Stefanov, G. Liu, A. Liashenko, P. Piskorz, I. Komaromi, R. L. Martin, D. J. Fox, T. Keith, M. A. Al-Laham, C. Y. Peng, A. Nanayakkara, M. Challacombe, P. M. W. Gill, B. Johnson, W. Chen, M. W. Wong, C. Gonzalez and J. A. Pople, *GAUSSIAN 03 (Revision C.02)*, Gaussian Inc., Wallingford CT, 2004.
39 C. Gonzalez and H. B. Schlegel, *J. Chem. Phys.*, 1989, **90**, 2154.
40 C. Gonzalez and H. B. Schlegel, *J. Phys. Chem.*, 1990, **94**, 5523.
41 R. Seeger and J. A. Pople, *J. Chem. Phys.*, 1977, **66**, 3045.
42 M. Stein and W. Lubitz, *J. Inorg. Biochem.*, 2004, **98**, 862.
43 C. Stadler, A. L. de Lacey, Y. Montet, A. Volbeda, J. C. Fontecilla–Camps, J. C. Conesa and V. M. Fernandez, *Inorg. Chem.*, 2002, **41**, 4424.
44 S. E. Lamle, S. P. J. Albracht and F. A. Armstrong, *J. Am. Chem. Soc.*, 2005, **127**, 6595.
45 J. Coremans, C. J. van Garderen and S. P. J. Albracht, *Biochim. Biophys. Acta.*, 1986, **883**, 145.
46 J. Coremans, C. J. van Garderen and S. P. J. Albracht, *Biochim. Biophys. Acta.*, 1992, **1119**, 157.

